Genomic blueprint of a relapsing fever pathogen in 15th century Scandinavia

Meriam Guellil[a,1], Oliver Kersten[a], Amine Namouchi[a], Egil L. Bauer[b], Michael Derrick[b], Anne Ø. Jensen[b], Nils C. Stenseth[a,1], and Barbara Bramanti[a,c,1]

[a]Centre for Ecological and Evolutionary Synthesis, Department of Biosciences, University of Oslo, N-0316 Oslo, Norway; [b]Norwegian Institute for Cultural Heritage Research, N-0155 Oslo, Norway; and [c]Department of Biomedical and Specialty Surgical Sciences, Faculty of Medicine, Pharmacy and Prevention, University of Ferrara, 35-441221 Ferrara, Italy

Contributed by N. C. Stenseth, August 13, 2018 (sent for review May 4, 2018; reviewed by Sally J. Cutler and Albert R. Zink)

Louse-borne relapsing fever (LBRF) is known to have killed millions of people over the course of European history and remains a major cause of mortality in parts of the world. Its pathogen, *Borrelia recurrentis*, shares a common vector with global killers such as typhus and plague and is known for its involvement in devastating historical epidemics such as the Irish potato famine. Here, we describe a European and historical genome of *B. recurrentis*, recovered from a 15th century skeleton from Oslo. Our distinct European lineage has a discrete genomic makeup, displaying an ancestral *oppA-1* gene and gene loss in antigenic variation sites. Our results illustrate the potential of ancient DNA research to elucidate dynamics of reductive evolution in a specialized human pathogen and to uncover aspects of human health usually invisible to the archaeological record.

ancient genomics | relapsing fever | vector-borne pathogen | immune evasion | aDNA

Louse-borne relapsing fever (LBRF), once one of many fevers ravaging Europe, has disappeared from the Western world and is now endemic to only eastern Africa. The disease is part of a group of well-known deadly louse-borne pathogens, which specialize in vector–human transmission. Its causative pathogen is the spirochete *Borrelia recurrentis*, whose only known vector is the human body louse, *Pediculus humanus*. This sets it apart from other tick-borne relapsing fever (TBRF) pathogens, such as its most closely related strains *Borrelia duttonii* and *Borrelia crocidurae* (1, 2).

Genomes of the genus *Borrelia* are unique. They are composed of up to 24 circular and linear plasmids with covalently closed hairpin telomeres showcasing AT-rich genomes of very small sizes. While the chromosomes, generally around 900–930 kbp, are very conserved across species, a high level of DNA rearrangements can be found among the plasmids (3–5), with some carrying essential genes, such as the telomere resolvase gene *resT* on plasmid pl23 of *B. recurrentis* and *B. duttonii*.

The *B. recurrentis* genome (1.24 Mbp) is composed of one linear chromosome and seven linear plasmids and is characterized by its low GC content (mean 28.1%). Genomic and ecological data on the pathogen are scarce, since it is challenging to cultivate and studies lack an animal model (6, 7). Research on the pathogen has therefore been limited to clinical samples, resulting thus far in the publication of one deposited reference sequence, strain A1 (5), and six additional datasets from eastern African strains (8).

LBRF is fatal in 10–40% of untreated cases (9) and is transmitted from vector to host when the hemocoel of crushed lice comes into contact with intact mucosa or skin (9). Studies (10) have also suggested a possible transmission of LBRF via lice feces. Like all relapsing fevers (RF), it is characterized by multiple febrile episodes separated by short periods of remission. Defining symptoms of LBRF are epistaxis and jaundice (9).

The disease was first mentioned in medical texts by Hippocrates from the fourth century BCE, in which he describes a series of fevers afflicting the populations of Thasos after a harsh winter (11). Further references to LBRF can be found throughout European history with prominent examples being outbreaks during the Great Irish Famine of 1846–1852 (11–13) and the post-World War I pandemic (1919–1923), which is estimated to have killed more than five million people in central Europe and Russia alone (14, 15). It has also been hypothesized that the so-called "pestis flava" or "Buidhe Chonaill" of sixth century CE Ireland was an LBRF epidemic (16). LBRF frequently emerged with typhus, which is also louse-borne and caused by the bacterium *Rickettsia prowazekii* (12).

Today, outbreaks of the disease can be found sporadically in Ethiopia, Eritrea, Somalia, and Sudan, where it is still endemic and until recently was the fifth most common cause of death (17). In addition to recent European reports of the disease among refugees (18), which clearly highlight how quickly a decline in hygiene and living conditions can lead to the spread of LBRF, a study by Brouqui et al. (19) detected a clear increase of individuals with IgG antibodies for LBRF in 2000 and 2002. The study therefore suggests that small, undetected outbreaks of the disease still exist to this day in European populations exposed to body lice infestation.

While LBRF is the only known RF capable of reaching epidemic proportions, it was never possible to confirm the presence

Significance

Louse-borne relapsing fever was one of the major diseases affecting Western human populations, with its last major pandemic killing millions after World War I. Despite the major role fevers have played in epidemic events throughout history, molecular evidence for the presence of their etiological agent has been extremely scarce in historical samples worldwide. By comparing our medieval *Borrelia recurrentis* genome with modern representatives of the species, we offer an historical snapshot of genomic changes in an immune-evasion system and of reductive evolution in a specialized vector-borne human pathogen. This shotgun sequencing project highlights the potential for ancient DNA research to uncover pathogens which are undetectable to osteological analysis but are known to have played major roles in European health historically.

Author contributions: M.G. designed research; M.G. and O.K. collected data; M.G., O.K., and A.N. performed research; M.G. analyzed data; E.L.B, M.D., and A.Ø.J. provided archaeological/osteological information; and M.G., O.K., E.L.B., M.D., A.Ø.J., N.C.S., and B.B. wrote the paper.

Reviewers: S.J.C., University of East London; and A.R.Z., EURAC Research.

The authors declare no conflict of interest.

Data deposition: Sequencing data have been deposited at the European Nucleotide Archive (accession no. PRJEB24501).

[1]To whom correspondence may be addressed. Email: meriam.guellil@ibv.uio.no, n.c.stenseth@ibv.uio.no, or barbara.bramanti@ibv.uio.no.

This article contains supporting information online at www.pnas.org/lookup/suppl/doi:10.1073/pnas.1807266115/-/DCSupplemental.

of the pathogen in archaeological samples. Previous attempts at detecting *B. recurrentis* in archaeological samples have been unsuccessful (20, 21) but have succeeded in detecting other louse-borne pathogens such as the typhus agent *R. prowazekii*. The only previously reported ancient DNA (aDNA) sequences of the genus *Borrelia* came from the Tyrolean Iceman Ötzi (22), who carried sequences matching the Lyme disease pathogen *Borrelia burgdorferi*.

Results

Skeleton OSL9/SZ50522 (Fig. 1*A*) was found during the excavation of a graveyard south of St. Nicolay's Church, in Oslo (Fig. 1*B*, *SI Appendix*, and *SI Appendix*, Fig. S1) (23). It was part of a double burial (SA50521) situated close to the southern boundary of the graveyard and was identified as a female individual (age 28–35 y) who had been buried with a child (age 7–9 y) (24). A rib fragment was radiocarbon dated to Cal CE 1430–1465 (*SI Appendix*, Fig. S2 and Table S1).

The initial metagenomic analysis of shotgun sequencing data from individual OSL9/SZ50522 revealed hits matching the spirochete *B. recurrentis*. After mapping the data to the *B. recurrentis* A1 genome assembly, we recovered 16.9% of the chromosome with a mean depth of coverage below 1 and deamination patterns matching aDNA.

To assemble the medieval *B. recurrentis* strain at an adequate depth and to cover more of the reference sequence, we sequenced 13 additional genomic libraries from two teeth (A+B) (*SI Appendix*, Fig. S3) over four lanes on a HiSeq 2500 Illumina system and generated *ca*. 1.2 billion raw DNA sequences (Dataset S8). Overall, each library contained less than 0.04% reads mapping to *B. recurrentis* (Dataset S4).

We were able to assemble a *B. recurrentis* genome at a mean depth of 6.4× with 95.2% of the genome being covered at least twice (Dataset S7), with a total of 152,490 reads mapping to *B. recurrentis* (Dataset S4). Ultimately, we were able to assemble 98.2% of the chromosome at a mean depth of coverage of 8.3× (Fig. 2*A*).

The read-length distribution (mean: 69 bp) (*SI Appendix*, Fig. S9) of all datasets showed that the DNA was in a highly fragmented state. Consistent with aDNA, we could also detect significant DNA damage patterns for the reads mapping to the *B. recurrentis* A1 assembly (Fig. 2*B* and *SI Appendix*, Fig. S5). This was further supported by the identification of a northern European mtDNA haplogroup and the DNA damage profile of the reads mapping to the revised Cambridge reference sequence (rCRS) build of the human mitochondrion (*SI Appendix* and *SI Appendix*, Fig. S6).

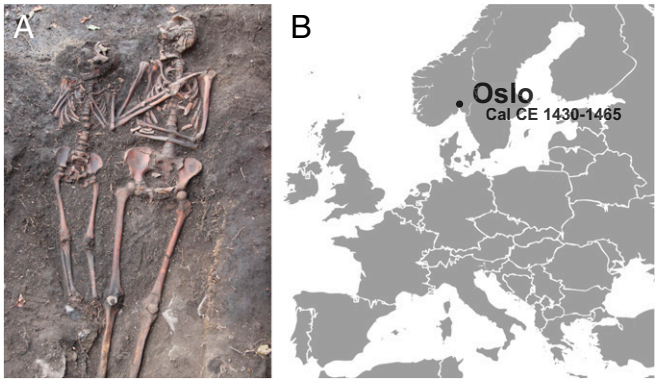

Fig. 1. Sample origin and site location. (*A*) In situ picture of the double burial SA50521 with individual OSL9/SZ50522 to the right. (*B*) Location of the archaeological site and C14 date of the burial displayed in *A*.

The unique genomic structure of these highly specialized bacteria allows high mapping specificity across the *B. recurrentis* genome (4, 5). This, in turn, allows us to infer the presence and absence of genomic regions via the level of coverage observed after mapping the raw datasets to *Borrelia* references. Additionally, the use of a shotgun dataset, as opposed to a target-enrichment sequencing strategy, did not restrict or shift the available data to known preselected modern sequences.

To ascertain that the organism represented in our metagenomic output was in fact a *B. recurrentis* strain and not one of its most closely related species, and potentially to detect signs of plasmid rearrangements, we mapped all datasets against available reference sequences for *B. duttonii* Ly and *B. crocidurae* Achema independently (Fig. 2*C* and *SI Appendix*, Fig. S4). The number of reads mapping to the chromosomal assemblies varies only slightly from one species to another, but we observe distinctly higher numbers of reads mapping with edit distance 0 to the *B. recurrentis* genome than to any of the other genomes (Fig. 2*D* and *SI Appendix*, Fig. S7 and Dataset S5).

Most *B. recurrentis* plasmids are colinear to *B. duttonii* plasmids with the exception of pl6, which is colinear to a 5-kbp plasmid in *B. crocidurae*. While pl6 is covered at a mean depth of coverage of 12.6× in our genome mapping, we clearly observed that noncolinear plasmids of *B. duttonii* and *B. crocidurae* are not present in our medieval strain (*SI Appendix*, Fig. S4).

Six newly published de novo genomes by Marosevic et al. (8) stemming from Eastern African refugees treated for relapsing fever seem to have reinforced previously raised doubts (25) regarding the length of plasmids pl124 and pl6 (NC_011263.1). The new strains all exhibit a *ca*. 40-kbp extension at the 5′ end of the previously reported pl124 and a *ca*. 1-kbp reduction at the 3′ end of pl6, much like their respective colinear plasmids pl165 in *B. duttonii* and a 5-kbp-long plasmid in *B. crocidurae*. Interestingly, our ancient *B. recurrentis* genome also displays signs of a longer pl124 and a shorter pl6 (*SI Appendix*, Figs. S4*A* and S10) compared with the reference strain A1. Our mapping to pl6 was completely missing 1 kbp at the 3′ end of the plasmid. Similarly, while aligning our data to pl165 of *B. duttonii*, we observed uniform mapping at a mean depth of coverage of 3× across the entire length of the plasmid, including the missing 40-kbp extension at the 5′ end. It is highly likely that these discrepancies can be linked to the deposition of an incomplete assembly of the original reference genome strain A1, since both our medieval European strain and the modern African strains show the same variations. This was further validated by pulse-field gel electrophoresis and the amplification of a gene ortholog to *cihC* in *B. duttonii* at 27,465–28,535 bp (26).

Upon further inspection of the plasmids, we found that three identical 582-bp-long variable short proteins (vsp) genes are missing at the 3′ end of plasmids pl33, pl37, and pl53 (Fig. 3). Strikingly, these genes mark the end of mapping for plasmid pl33 and pl37, while pl53 retains a hypothetical protein at its 3′ end. The first *ca*. 130 bp at the 5′ end of the vsp gene are covered by nonunique reads restricted to the gene across all three plasmids. This indicates that pl33, pl37, and pl53 are shorter in strain OSL9 and that we could be seeing signs of undetected plasmid rearrangements involving a similar vsp gene. The genes missing after the 582-bp vsp genes are copies of five variable long proteins (vlp) genes and multiple hypothetical proteins. Identical copies of a 785-bp-long vlp pseudogene are missing across all three plasmids, with the copy on pl33 being only 475 bp long. While the deposited assembly of this plasmid is known to be missing parts of its telomeric sequence, it might also be missing the end of the 785-bp vlp pseudogene and one or more of the four additional identical vlp pseudogenes missing across pl37 and pl53 (Fig. 3 and Dataset S2).

Additionally, plasmids pl37 and pl53 have a decreased coverage in the intervals 23,822–28,471 and 39,440–44,087 bp, respectively.

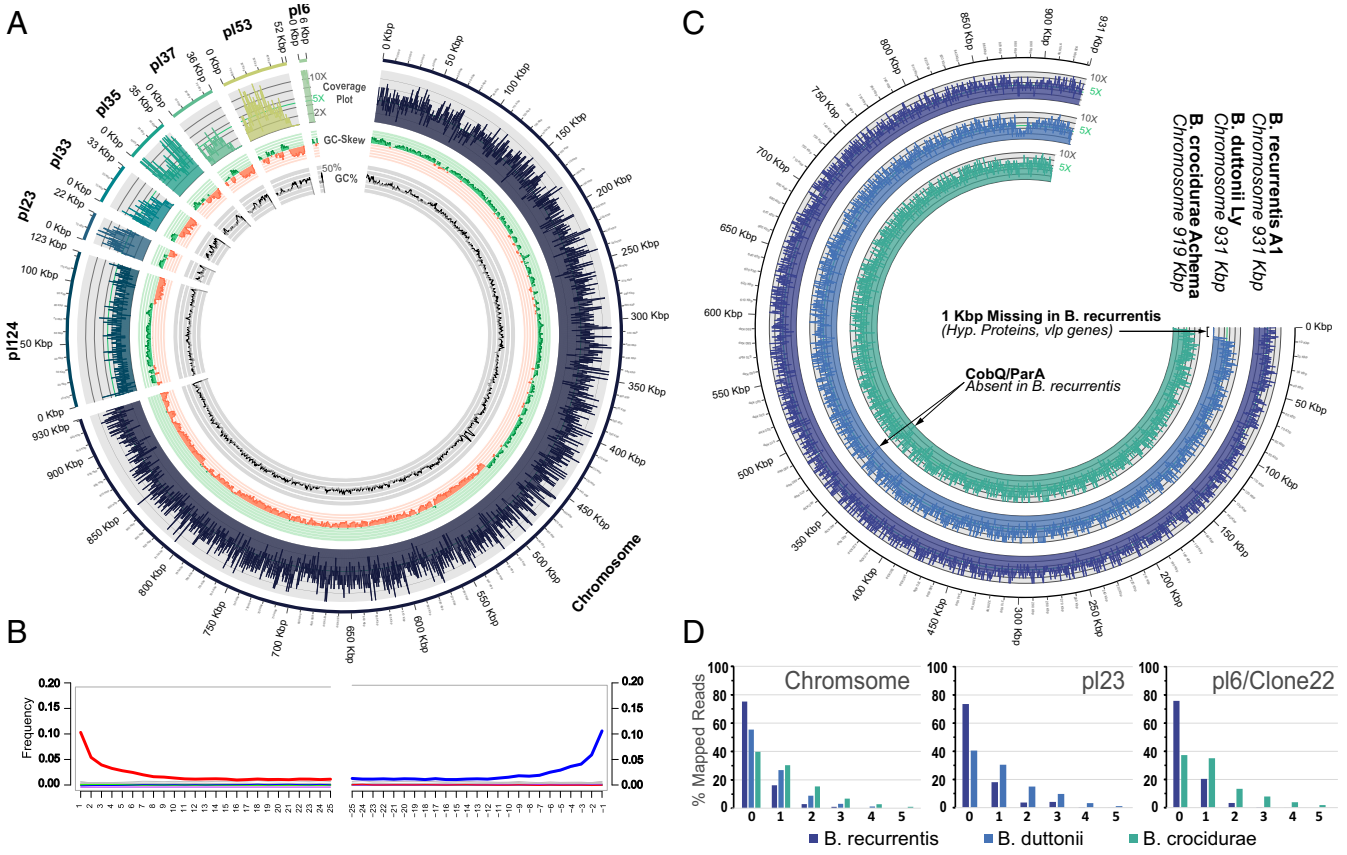

Fig. 2. (*A*) Coverage plots for mapping of OSL9A-B reads to the *B. recurrentis* A1 reference sequence. Rings (from outer ring to inner ring) show coverage, GC skew, and GC content. GC content is further highlighted as being above (black) or below (gray) 26%. (*B*) Damage frequency for the mapping displayed in *A* with 10% of reads showing a clear deamination signature consistent with aDNA. (*C*) Comparison of OSL9A-B noncompetitive mappings to the chromosomes of *B. recurrentis* A1, *B. duttonii* Ly, and *B. crocidurae* Achema. It can be seen here that strain OSL9 does not have a CobQ/ParA gene and is also missing a 1-kbp-long sequence at the 5′ end of the *B. duttonii* chromosome, much like *B. recurrentis* A1. (*D*) Distribution of edit distances (plotted on the *x* axis) of OSL9A-B reads mapping to chromosomal assemblies of *B. recurrentis* A1, *B. duttonii* Ly, and *B. crocidurae* Achema (*Left*), to colinear pl23 plasmids of *B. recurrentis* A1 and *B. duttonii* Ly (*Center*), and to colinear pl6 plasmids of *B. recurrentis* A1 and *B. crocidurae* Achema (*Right*).

The sequences are both 4,648 bp long and share 99% identity over their entire length. These intervals distinguish themselves by a patchy and low coverage, with most vlp and vsp genes in the region being covered *ca*. 50–80% (mean coverage 75.2%), while the covered vlp and vsp genes outside these intervals show a mean coverage of 96.9%, hinting at potential sequence degradation or plasmid rearrangements. Overall, 11 vlp pseudogenes and three vsp genes are missing, with one additional vsp pseudogene and three vlp genes showing signs of potential degradation.

We investigated the presence of known frameshift and stop-gain mutations throughout our ancient genome and found that, with the exception of *oppA-1*, all pseudogenes, which *B. recurrentis* A1 acquired during its reductive evolution and divergence from *B. duttonii* Ly, were present in the medieval strain. Our alignments to both *B. recurrentis* A1 and *B. duttonii* Ly support (depth of coverage 5×) that the *oppA-1* gene could still be active in the OSL9 strain by retaining its ancestral glutamine (residue 59) (*SI Appendix*, Fig. S8).

After aligning all OSL9A-B reads to the chromosome of the reference strain, *B. recurrentis* A1, we detected 321 SNPs (Dataset S3). These SNPs were then combined with all other SNPs found in RF *Borrelia* strains included in this study to build a phylogenetic tree using the maximum likelihood method. Before building the phylogeny, we checked for the presence of recombination using a phi test and ClonalFrameML software but could not detect any sign of recombination, as these approaches yielded a *P* value of 0.8287 and a likelihood of −612.47, respectively. The midpoint-rooted tree was generated using PhyML. The phylogeny clearly shows two clusters represented by LBRF and TBRF species (Fig. 4), and, as previously reported, the African RF isolates cluster together (8). Interestingly, the ancient genome recovered in Oslo is clustered between *B. duttonii* and the African *B. recurrentis* strains in the phylogeny. Compared with all other *Borrelia* in this study, 164 SNPs are specific to the OSL9 strain. These SNPs are distributed as 77 nonsynonymous SNPs, 77 synonymous SNPs, and 10 intergenic SNPs.

Discussion

LBRF is characterized by multiple relapses of fever, which are believed to be caused by bacterial immune evasion systems. RF *Borreliae* use plasmid-encoded antigenic phase variation within a clonal population as a mechanism of immune evasion. It utilizes the sequential expression of different variants of an antigenic surface protein to evade the host immunity, prolong the infection, and promote transmission. Hence, each new wave of infection, in this case febrile relapse, is characterized by a new serotype (5, 6, 27–29). In *B. recurrentis*, these proteins are the surface lipoproteins vlp and vsp, which are also known to be its main proinflammatory proteins (30). The genes expressing these proteins are arranged across plasmids in silent and expressed copies, and the interaction between the host immunity and the phase-variation mechanism encoded in the pathogen's genome are believed to be responsible for the febrile relapses of LBRF (29). The number of phase-variation loci or loci families dictates the number of possible serotypes and, thus, the number of genome variants theoretically available to evade the host immunity,

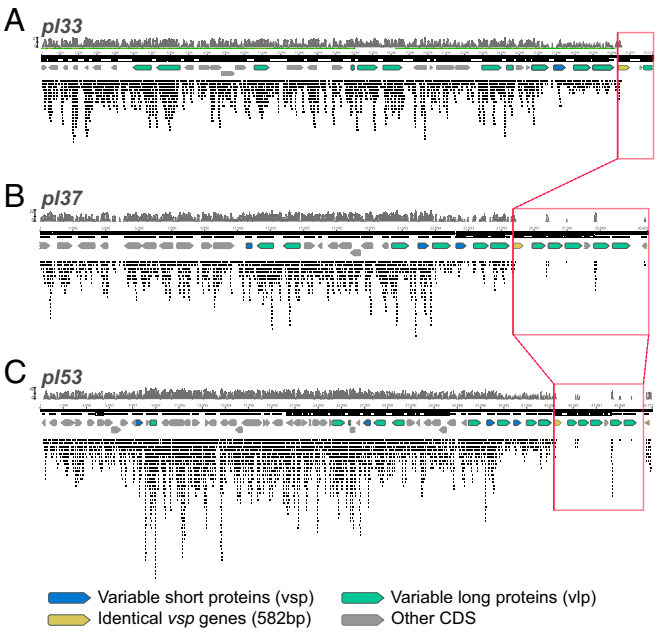

Fig. 3. Alignment of OSL9A-B reads to *B. recurrentis* plasmids pl33 (*A*), pl37 (*B*), and pl53 (*C*). Across all plasmids a section at the 3′ end of the linear plasmids is missing starting with 80% of a vsp gene. The regions boxed in red share identities of 99–100%. Tiled reads seen within the boxed regions are nonunique reads mapping to sequences conserved across multiple plasmids.

with some estimating up to 2^{10} different states for every 20 phase-variation sites (28, 29, 31). As a result, although LBRF can be treated with antibiotics, no vaccine against the disease exists today. The only effective antibodies against LBRF seem to be directed at vlp and vsp genes and thus only can be manufactured to fight one randomly appearing serotype at a time (32).

We observed that a number of vlp and vsp genes are absent or potentially degraded in our medieval strain (Fig. 3 and Dataset S2), but are present in modern-day African strains and have orthologs in other RF genomes. Some are frameshifted or incomplete in A1 and might have been pseudogenes, but others, like the vsp copies found at the beginning of each missing interval, were fully functional genes. We can hypothesize, based on the data at hand, that the observed loss of antigenic phase-variation loci could have led to a difference in phenotype compared with modern strains and hypothetically could have influenced the number of febrile relapses, i.e., the number of serotypes that the medieval strain of the pathogen might have been capable of generating. While experimental infections by LBRF have yielded up to 10 relapses (9, 32), most sources cite up to five relapses for the pathogen (33). Similarly, most untreated non-European cases recorded during the World War I/World War II pandemics reached only up to five relapses (11, 34). Historically, Creighton (12) recorded varying numbers of observed relapses across known LBRF outbreaks. An outbreak in 18th century Dublin cites that patients were prone to relapses "even sometimes to the third" (35). Overall, most outbreaks, for which the number of observed relapses was supplied in historical texts, saw one or two or "one or more" relapses. However, it should be noted that data on modern untreated cases of LBRF are rare, and most available historical sources only refer to "multiple relapses" or "prone to relapse" (12, 36), considerably reducing the amount of data to be evaluated (36).

Compared with *B. duttonii* Ly, the modern reference strain *B. recurrentis* A1 has lost a large number of intact vlps and vsps and causes fewer relapses in human patients (5, 33), but this difference is even more pronounced in the medieval strain. The missing genes make up all archival copies of six phase-variation loci. Overall, this translates to a genome reduction of 1.2% of the pan-genome and 5.1–21% of the affected plasmids, which, in combination with a decrease in GC content (Dataset S4), is in line with observed reductive genome evolution of specialized and highly pathogenic bacteria (37, 38). The presence of additional unknown plasmids seems unlikely, as the number of plasmids tends to follow the same reductive trend as the overall genome (37). Instead, we can detect additional gene loss at the 3′ end of some plasmids.

This reductive evolution characterizes *B. recurrentis*' epidemic potential and its increased virulence compared with other RFs. Similar to *Bartonella quintana* and *Rickettsia prowazekii* (38, 39), other well-known body lice-to-human transmission specialists, *B. recurrentis* shows accelerated rates of genome degradation caused by adaptation to host-restricted vectors and functional trade-offs, resulting in a degraded genome, reduced genome size, low coding content, and increased virulence (5, 31, 37, 38).

However, this type of evolution usually involves the loss of regulatory genes (37), and while this is also the case for our medieval strain, there is one exception. The oppA operon, which encodes for an ABC transporter, is significantly involved in the uptake of oligopeptides in many bacterial species (40, 41). *OppA-1*, which likely plays a critical role in host environment adaptation and essential metabolic functions (42), is a pseudogene in *B. recurrentis* A1 due to an in-frame stop codon. However, our medieval strain retains the ancestral glutamine much like the TBRF pathogen *B. duttonii*. While we can only speculate about the effect of this mutation on the ecological life cycle of the disease, it is interesting to note that the inactivation of *oppA-1* seems to be much more recent than the rest of the pseudogenes in *B. recurrentis*. These pseudogenes are degraded to the same extent in both *B. recurrentis* lineages, with the exception of some antigenic phase-variation loci, which the medieval strain seems to have lost altogether. Therefore, we could hypothesize that, while both lineages have continued their reductive evolution, they have done so in different ways.

The full ecological dynamics of LBRF remain unclear (43). The European lineage presented in this study probably evolved in a distinctly different environment than known modern African strains. The extent to which anthropogenic pressure on pathogen and vector impacted this evolution is difficult to assess based on a single representative in the medieval lineage. As the only epidemic and louse-borne RF, LBRF has been assumed to be responsible for all RF epidemics recorded throughout European

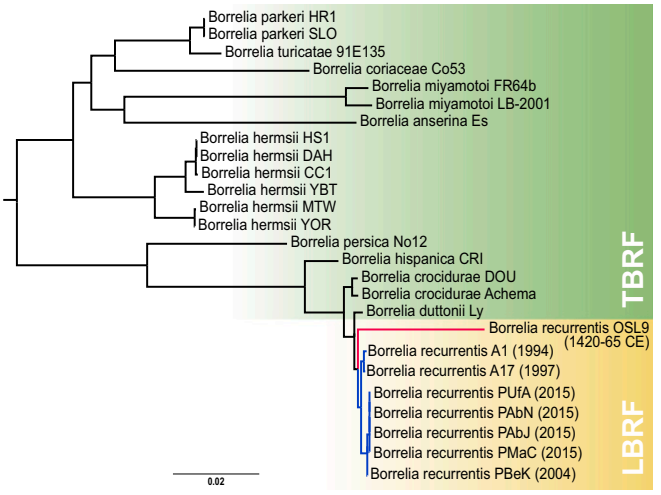

Fig. 4. RL phylogeny based on chromosomal alignments (Datasets S3 and S9). The European LBRF strain (this study) is shown in red, and African LBRF strains are shown in blue. The legend displays the branch length.

history. It was known to have reached epidemic proportions in susceptible populations around key events, such as wars and famines. LBRF is a disease that probably would only infrequently have resulted in the type of mass mortality that would warrant the planning of mass graves, and, historically, scattered cases of LBRF have been recorded between epidemics, usually among the poor (12). Although at the time of the burial of individual OSL9/SZ50522 the town was still affected by the economic decline caused by the Black Death in the mid-1300s (44, 45), which probably left parts of the population vulnerable to disease and malnourishment, the results reported in this study represent an isolated case of the disease. Given the available data, we cannot speculate on the presence or size of an outbreak of LBRF in 15th century Oslo, especially since the number of studied samples from the same time period is limited (Dataset S1). However, our results can tentatively corroborate the involvement of *B. recurrentis* in the European epidemics reported in historical text because of its being the only known epidemic RF, the specificity of the reported symptoms, the identification of the spirochete during epidemics in 1868, and the discovery of its relation to lice in 1907 (33, 46). Finally, the studied individual probably died at the height of bacteremia, allowing the detection of the pathogen in relatively high quantities within aDNA shotgun datasets.

Previously assembled ancient pathogens have generally been limited to diseases that could leave visible marks on the skeletons or mummified tissues of affected individuals (e.g., leprosy, tuberculosis, smallpox) (47–49). However, recent studies on pathogens that are invisible in the archaeological record have started to emerge (48, 50, 51). These studies are of particular relevance, as they clearly illustrate the osteological paradox (52, 53). It is hoped that, as one of the few epidemic fevers believed to have played a major role in the disease landscape of historical Europe, the addition of LBRF will lead the way for the detection of diseases which might not have much relevance to Western health today and therefore are less represented in the genomic databases and literature. The unique genome of *B. recurrentis* has provided a rare opportunity in aDNA to study the genomic make-up of an ancient pathogen and catch a glimpse of the evolutionary process that accompanies the environmental adaptation and pathogenesis of specialized human pathogens. Furthermore, the results detailed in our study illustrate the importance of human body lice as a vector throughout European history, which has recently also been suggested for plague (54).

Future research into the ecological dynamics of LBRF and surveillance of populations affected by lice infestation in industrialized countries is needed to better understand the persistence mechanism of the disease and the dangers of spread in susceptible Western communities. Furthermore, more insights into potential outbreaks of the disease in lice-infested Western populations, as seen in Brouqui et al. (19), and genomic sequences from affected patients would allow us to determine if LBRF persisted in Europe and thus is phylogenetically related to the lineage recovered in this study or was imported on one or more occasions from outside Europe. Additional genomes, European or otherwise, may further elucidate the evolution and pathogenicity of LBRF.

Methods

Samples. We sampled two well-preserved molars from nine individuals (Dataset S1) recovered from the site of St. Clement's/St. Nicolay's church graveyard in Oslo, under clean conditions at the Norwegian Institute for Cultural Heritage Research, Oslo. One exception was tooth OSL6B, which was an incisor. The individuals all stem from different periods of the graveyard, which spans the 11th to the 15th century (Dataset S1). Upon discovery of *B. recurrentis* reads in OSL9, all sampled individuals were screened for the presence of the pathogen via qPCR but were negative (*SI Appendix*, Fig. S3), including the only potentially contemporary individual OSL6/SZ19834.

Laboratory Work. Full experimental procedures are provided in *SI Appendix*.

Data Preparation and Quality Filtering. Following sequencing, the datasets were demultiplexed at the Norwegian Sequencing Centre, and quality control was performed using FastQC (55). Adapters and indices were trimmed using cutadapt2.0 (56). Sequences shorter than 30 bp and below a quality score of 10 were discarded. Trimmed reads were merged using FLASH (57).

Metagenomic Analysis. The datasets were explored using the taxonomic classifier Kraken (58). Upon discovery of *B. recurrentis* reads, we further investigated the metagenomic data using MetaPhlAn2 (59) and the protein-level classification tool Kaiju (60). All tools indicated the presence of the bacterium in all datasets stemming from individual OSL9/SZ50522. No hits for *B. recurrentis* were found in any other samples or blank controls.

RF Borreliae Mappings. The merged reads were mapped noncompetitively to the *Borrelia recurrentis* A1 strain (ASM1970v1), *Borrelia duttonii* Ly strain (ASM1968v1), and *Borrelia crocidurae* Achema strain (ASM25934v1) reference sequences using BWA-ALN (-n 0·01 -l 16500) and BWA Samse (61). The generated data were converted to bam format and sorted using SAMtools (62, 63). Duplicates were marked using Picard MarkDuplicates module (64). Indels were realigned using GATK RealignerTargetCreator and IndelRealigner modules (65, 66). Using mapDamage2.0 (67), we quantified aDNA damage patterns for each dataset and recalibrated the quality scores of likely damaged bases. Libraries from tooth B yielded significantly more sequences mapping to *B. recurrentis* than libraries from tooth A, with an average 11,346 reads per dataset mapping to the reference compared with an average of 3,402 reads per dataset for tooth A.

Phylogeny. Species for which only contigs were available were assembled with Multi-CAR (68) using the reference sequences for *B. recurrentis* A1 and *Borrelia hermsii* HS1. For six recently published *B. recurrentis* strains (8), we mapped available Illumina reads to the *B. recurrentis A1* chromosome assembly using BWA-MEM, sorted the data with SAMtools (62), marked duplicates using Picard (64), and realigned around indels with GATK (65, 66). For all BAM files, SNPs were called with SAMtools mpileup (-R -ugf -B) and BCFtools call (-vm) and filter (-s LOWQUAL -i '%QUAL > 19'). SNPs were annotated using snpToolkit (69). Complete genomes were compared using Parsnp (70), and polymorphic sites were extracted using gingr. Two methods, Phi test (71) and ClonalFrameML (72), were used to assess the presence of recombination in our dataset. The midpoint-rooted tree was generated using phyML.

ACKNOWLEDGMENTS. Data analysis was performed on the Abel Cluster owned by the University of Oslo and the Norwegian Metacenter for High Performance Computing and operated by the Department for Research Computing at USIT, the University of Oslo information technology department. Skeletal material was provided courtesy of the Museum of Cultural History (University of Oslo) after application to the museum and the Norwegian National Committee for Research Ethics on Human Remains. This project was funded by the European Research Council under FP7-IDEAS-ERC Program Grant 324249 MedPlag.

1. Elbir H, et al. (2012) Complete genome sequence of Borrelia crocidurae. *J Bacteriol* 194:3723–3724.
2. Fotso Fotso A, et al. (2014) Genome sequence of Borrelia crocidurae strain 03-02, a clinical isolate from Senegal. *Genome Announc* 2:e01150-14.
3. Gupta RS, Mahmood S, Adeolu M (2013) A phylogenomic and molecular signature based approach for characterization of the phylum spirochaetes and its major clades: Proposal for a taxonomic revision of the phylum. *Front Microbiol* 4:217.
4. Norris SJ, Lin T (2011) Out of the woods: The remarkable genomes of the genus Borrelia. *J Bacteriol* 193:6812–6814.
5. Lescot M, et al. (2008) The genome of Borrelia recurrentis, the agent of deadly louse-borne relapsing fever, is a degraded subset of tick-borne Borrelia duttonii. *PLoS Genet* 4:e1000185.
6. Vidal V, Cutler S, Scragg IG, Wright DJM, Kwiatkowski D (2002) Characterisation of silent and active genes for a variable large protein of Borrelia recurrentis. *BMC Infect Dis* 2:25.
7. Cutler SJ, et al. (1997) Borrelia recurrentis characterization and comparison with relapsing-fever, Lyme-associated, and other Borrelia spp. *Int J Syst Bacteriol* 47: 958–968.

8. Marosevic D, et al. (2017) First insights in the variability of Borrelia recurrentis genomes. *PLoS Negl Trop Dis* 11:e0005865.
9. European Centre for Disease Prevention and Control (2017) Facts about louse-borne relapsing fever ecdc. Available at https://ecdc.europa.eu/en/louse-borne-relapsing-fever/facts. Accessed August 8, 2017.
10. Houhamdi L, Raoult D (2005) Excretion of living Borrelia recurrentis in feces of infected human body lice. *J Infect Dis* 191:1898–1906.
11. Bryceson A, et al. (1969) Louse-borne relapsing fever; a clinical and laboratory study of 62 cases in Ethiopia and a reconsideration of the literature. Naval Medical Research Unit No 3 APO New York 09319 Field Facility. Available at www.dtic.mil/docs/citations/AD0722494. Accessed July 12, 2017.
12. Creighton C (1894) *A History of Epidemics in Britain: From the Extinction of Plague to the Present Time* (Cambridge Univ Press, Cambridge, UK).
13. Hays JN (2005) "Fevers" and the Great famine in Ireland, 1846–1850. *Epidemics and Pandemics: Their Impacts on Human History*, ed Hays JN (ABC CLIO Santa Barbara, CA), pp 439–448.
14. Sparrow H (1958) Etude du foyer éthiopien de fièvre récurrente. *Bull World Health Organ* 19:673–710.
15. Sparrow H (1962) Tropical Health: A Report on a Study of Needs and Resources. (National Academies, Washington, DC).
16. Macarthur W (1948) Famine fevers in England and Ireland. *Ulster Med J* 17:28–33.
17. Cutler SJ (2010) Relapsing fever–A forgotten disease revealed. *J Appl Microbiol* 108: 1115–1122.
18. European Centre for Disease Prevention and Control (2015) Rapid Risk Assessment: Louse-borne relapsing fever in the EU – 17 November 2015 (ECDC Stockholm). Available at https://ecdc.europa.eu/sites/portal/files/media/en/publications/Publications/louse-borne-relapsing-fever-in-eu-rapid-risk-assessment-17-nov-15.pdf. Accessed June 30, 2017.
19. Brouqui P, et al. (2005) Ectoparasitism and vector-borne diseases in 930 homeless people from Marseilles. *Medicine (Baltimore)* 84:61–68.
20. Tran T-N-N, et al. (2011) High throughput, multiplexed pathogen detection authenticates plague waves in medieval Venice, Italy. *PLoS One* 6:e16735.
21. Nguyen-Hieu T, et al. (2010) Evidence of a louse-borne outbreak involving typhus in Douai, 1710-1712 during the war of Spanish succession. *PLoS One* 5:e15405.
22. Keller A, et al. (2012) New insights into the Tyrolean Iceman's origin and phenotype as inferred by whole-genome sequencing. *Nat Commun* 3:698.
23. Derrick M (2018) Follobaneprosjektet F04 Klypen Øst og Saxegaardsgata 15. *Arkeologisk Utgravning Mellom Bispegata og Loenga. Middelalderparken Og Saxegaardsgata 15 & 17, Oslo. NIKU Oppdragsrapport 40/2015* (Norsk institutt for kulturminneforskning, Oslo).
24. Jensen AØ (2018) Osteologisk analyse av skjelettmaterialet fra Nikolaikirkens kirkegård. *Follobaneprosjektet F04 Klypen Øst/Saxegaardsgata 15. NIKU Oppdragsrapport 160/2016* (Norsk institutt for kulturminneforskning, Oslo).
25. Miller SC, Porcella SF, Raffel SJ, Schwan TG, Barbour AG (2013) Large linear plasmids of Borrelia species that cause relapsing fever. *J Bacteriol* 195:3629–3639.
26. Grosskinsky S, et al. (2010) Human complement regulators C4b-binding protein and C1 esterase inhibitor interact with a novel outer surface protein of Borrelia recurrentis. *PLoS Negl Trop Dis* 4:e698.
27. Palmer GH, Bankhead T, Seifert HS (2016) Antigenic variation in bacterial pathogens. *Microbiol Spectr* 4.
28. Norris SJ (2006) Antigenic variation with a twist–The Borrelia story. *Mol Microbiol* 60: 1319–1322.
29. Foley J (2015) Mini-review: Strategies for variation and evolution of bacterial antigens. *Comput Struct Biotechnol J* 13:407–416.
30. Barbour AG, Restrepo BI (2000) Antigenic variation in vector-borne pathogens. *Emerg Infect Dis* 6:449–457.
31. Pallen MJ, Wren BW (2007) Bacterial pathogenomics. *Nature* 449:835–842.
32. Barbour AG, Guo BP (2010) Pathogenesis of relapsing fever. *Borrelia: Molecular Biology, Host Interaction and Pathogenesis*, eds Radolf JD, Scott Samuels D (Horizon Scientific, Norfolk, UK), pp 333–357.
33. Cutler SJ (2015) Relapsing fever Borreliae: A global review. *Clin Lab Med* 35:847–865.
34. Chung H-L, Chang FC (1939) Relapsing fever. clinical and statistical study of 337 cases. *Chin Med J* 55, 6–33.
35. Rutty J (1770) *A Chronological History of the Weather and Seasons, and of the Prevailing Diseases in Dublin: With Their Various Periods, Successions, and Revolutions, During the Space of Forty Years. With a Comparative View of the Difference of the Irish Climate and Diseases, and Those of England and Other Countries* (Robinson and Roberts, London).
36. Lyons RT (1872) *A Treatise on Relapsing or Famine Fever* (Henry S. King, London).
37. Diop A, Raoult D, Fournier P-E (December 27, 2017) Rickettsial genomics and the paradigm of genome reduction associated with increased virulence. *Microbes Infect*, 10.1016/j.micinf.2017.11.009.
38. Alsmark CM, et al. (2004) The louse-borne human pathogen Bartonella quintana is a genomic derivative of the zoonotic agent Bartonella henselae. *Proc Natl Acad Sci USA* 101:9716–9721.
39. Ogata H, et al. (2001) Mechanisms of evolution in Rickettsia conorii and R. prowazekii. *Science* 293:2093–2098.
40. Kornacki JA, Oliver DB (1998) Lyme disease-causing Borrelia species encode multiple lipoproteins homologous to peptide-binding proteins of ABC-type transporters. *Infect Immun* 66:4115–4122.
41. Wang X-G, Lin B, Kidder JM, Telford S, Hu LT (2002) Effects of environmental changes on expression of the oligopeptide permease (opp) genes of Borrelia burgdorferi. *J Bacteriol* 184:6198–6206.
42. Wang X-G, et al. (2004) Analysis of differences in the functional properties of the substrate binding proteins of the Borrelia burgdorferi oligopeptide permease (Opp) operon. *J Bacteriol* 186:51–60.
43. Amanzougaghene N, et al. (2017) Detection of bacterial pathogens including potential new species in human head lice from Mali. *PLoS One* 12:e0184621.
44. Nedkvitne A, Norseng PG (2000) *Middelalderbyen Ved Bjørvika. Oslo 1000-1536* (Cappelen, Oslo).
45. Unger CR, Huitfeldt-Kaas HJ, eds (1847) *Diplomatarium Norvegicum: Oldbreve Til Kundskab Om Norges Indre Og Ydre Forhold, Sprog, Slægter, Sæder, Lovgivning Og Rettergang I Middelalderen. Samling 11* (PT Mallings boghandels forlag, Christiania, Norway), Vol 5, p 835.
46. Southern PM, Sanford JP (1969) Relapsing fever: A clinical and microbiological review. *Medicine (Baltimore)* 48:129.
47. Kay GL, et al. (2015) Eighteenth-century genomes show that mixed infections were common at time of peak tuberculosis in Europe. *Nat Commun* 6:6717.
48. Patterson Ross Z, et al. (2018) The paradox of HBV evolution as revealed from a 16th century mummy. *PLoS Pathog* 14:e1006750.
49. Schuenemann VJ, et al. (2013) Genome-wide comparison of medieval and modern Mycobacterium leprae. *Science* 341:179–183.
50. Vågene ÅJ, et al. (2018) Salmonella enterica genomes from victims of a major sixteenth-century epidemic in Mexico. *Nat Ecol Evol* 2:520–528.
51. Kay GL, et al. (2014) Recovery of a medieval Brucella melitensis genome using shotgun metagenomics. *MBio* 5:e01337–e14.
52. Siek T (2013) The osteological paradox and issues of interpretation in paleopathology. *vis-à-vis: Explor Anthropol* 12:92–101.
53. Wood JW, et al. (1992) The osteological paradox: Problems of inferring prehistoric health from skeletal samples. *Curr Anthropol* 33:343–370.
54. Dean KR, et al. (2018) Human ectoparasites and the spread of plague in Europe during the Second Pandemic. *Proc Natl Acad Sci USA* 115:1304–1309.
55. Andrews S (2010) A quality control tool for high throughput sequence data. Available at https://www.bioinformatics.babraham.ac.uk/projects/fastqc/. Accessed August 14, 2017.
56. Martin M (2011) Cutadapt removes adapter sequences from high-throughput sequencing reads. *EMBnet J* 17:10–12.
57. Magoč T, Salzberg SL (2011) FLASH: Fast length adjustment of short reads to improve genome assemblies. *Bioinformatics* 27:2957–2963.
58. Wood DE, Salzberg SL (2014) Kraken: Ultrafast metagenomic sequence classification using exact alignments. *Genome Biol* 15:R46.
59. Segata N, et al. (2012) Metagenomic microbial community profiling using unique clade-specific marker genes. *Nat Methods* 9:811–814.
60. Menzel P, Ng KL, Krogh A (2016) Fast and sensitive taxonomic classification for metagenomics with Kaiju. *Nat Commun* 7:11257.
61. Li H, Durbin R (2009) Fast and accurate short read alignment with Burrows-Wheeler transform. *Bioinformatics* 25:1754–1760.
62. Li H, et al.; 1000 Genome Project Data Processing Subgroup (2009) The sequence alignment/map format and SAMtools. *Bioinformatics* 25:2078–2079.
63. Li H (2011) A statistical framework for SNP calling, mutation discovery, association mapping and population genetical parameter estimation from sequencing data. *Bioinformatics* 27:2987–2993.
64. Picard (2017) Available at broadinstitute.github.io/picard/. Accessed August 14, 2017.
65. DePristo MA, et al. (2011) A framework for variation discovery and genotyping using next-generation DNA sequencing data. *Nat Genet* 43:491–498.
66. Van der Auwera GA, et al. (2013) From FastQ data to high confidence variant calls: The Genome Analysis Toolkit best practices pipeline. *Curr Protoc Bioinformatics* 43: 11.10.1–11.10.33.
67. Jónsson H, Ginolhac A, Schubert M, Johnson PLF, Orlando L (2013) mapDamage2.0: Fast approximate Bayesian estimates of ancient DNA damage parameters. *Bioinformatics* 29:1682–1684.
68. Chen K-T, et al. (2016) Multi-CAR: A tool of contig scaffolding using multiple references. *BMC Bioinformatics* 17:469.
69. Namouchi A (2018) snpToolkit. Available at https://bitbucket.org/Amine-Namouchi/snptoolkit. Accessed June 26, 2018.
70. Treangen TJ, Ondov BD, Koren S, Phillippy AM (2014) The Harvest suite for rapid core-genome alignment and visualization of thousands of intraspecific microbial genomes. *Genome Biol* 15:524.
71. Bruen TC, Philippe H, Bryant D (2006) A simple and robust statistical test for detecting the presence of recombination. *Genetics* 172:2665–2681.
72. Didelot X, Wilson DJ (2015) ClonalFrameML: Efficient inference of recombination in whole bacterial genomes. *PLOS Comput Biol* 11:e1004041.